Chinese Chemical Letters 35 (2024) 108618

Contents lists available at ScienceDirect

Chinese Chemical Letters

journal homepage: www.elsevier.com/locate/cclet

Artificial stepwise light harvesting system in water constructed by quadruple hydrogen bonding supramolecular polymeric nanoparticles☆

Tangxin Xiao[a,*], Xiuxiu Li[a], Liangliang Zhang[a], Kai Diao[a,b], Zheng-Yi Li[a], Xiao-Qiang Sun[a], Leyong Wang[b,*]

[a] Jiangsu Key Laboratory of Advanced Catalytic Materials and Technology, School of Petrochemical Engineering, Changzhou University, Changzhou 213164, China
[b] Jiangsu Key Laboratory of Advanced Organic Materials, School of Chemistry and Chemical Engineering, Nanjing University, Nanjing 210023, China

ARTICLE INFO

Article history:
Received 11 February 2023
Revised 18 May 2023
Accepted 25 May 2023
Available online 26 May 2023

Keywords:
Light harvesting system
Supramolecular polymer
Quadruple hydrogen bonding
AIE
Self-assembly

ABSTRACT

Stepwise energy transfer is ubiquitous in natural photosynthesis, which greatly promotes the widespread use of solar energy. Herein, we constructed a supramolecular light harvesting system based on sequential energy transfer through the hierarchical self-assembly of **M**, which contains a cyanostilbene core flanked by two ureidopyrimidinone motifs, endowing itself with both aggregation-induced emission behavior and quadruple hydrogen bonding ability. The monomer **M** can self-assemble into hydrogen bonded polymers and then form supramolecular polymeric nanoparticles in water through a mini-emulsion process. The nanoparticles were further utilized to encapsulate the relay acceptor ESY and the final acceptor NDI to form a two-step FRET system. Tunable fluorescence including a white-light emission was successfully achieved. Our work not only shows a desirable way for the fabrication of efficient two-step light harvesting systems, but also shows great potential in tunable photoluminescent nanomaterials.

Natural photosynthesis provides an excellent example to harvest, transfer, and eventually convert solar energy to chemical energy [1,2]. During this process, the existence of a large number of antenna pigments, such as chlorophylls, in the chloroplast is indispensable for the initial collection of sunlight [3,4]. After that, the absorbed energy will go through multiple transfer steps to achieve the reaction center. Inspired by this, scientists have made a great effort to fabricate man-made light harvesting systems (LHSs) to study the fundamentals of energy harvesting and transfer, as well as the application of the excited energy [5–12]. Previous works mainly focus on constructing special scaffolds to accommodate antenna pigments (donors) and energy acceptors, as well as to avoid aggregation-caused quenching of these fluorophores. To this end, various scaffolds, such as metallacycles/cages/stacks [13–16], macrocycle-mediated nanoaggregates [17–23], DNAs [24,25], and peptides/proteins [26–28], have been extensively employed. Alternatively, aggregation-induced emission (AIE) [29,30] fluorophores offer another choice to act as antenna arrays since they show outstanding emissive properties in the aggregated state [31–35]. Subsequently, the construction of artificial LHSs based on AIE donor with Förster resonance energy transfer (FRET) processes have been highly attractable [36–43].

Supramolecular polymer is a kind of dynamic macromolecule which is formed by small-molecular-weight building blocks through non-covalent interactions [44–50]. Supramolecular polymerization is a powerful strategy to assist the formation of LHSs as it can bring the fluorophores together with efficient emission. For example, Yang and co-workers fabricated one-step energy transfer light harvesting supramolecular polymeric nanoparticles (SPNPs) through pillar[5]arene-based host-guest complexation [51]. Recently, Wang and co-workers constructed a sequential two-step energy transfer system through supramolecular copolymerization of three different σ-platinated (hetero)acenes driven by π-stacking interaction [52].

It is noteworthy that quadruple hydrogen bonding interaction based on ureidopyrimidinone (UPy) is a milestone in the development of supramolecular polymers [53–56]. Based on our experience on supramolecular self-assembly [57–60] and a recent work on one-step LHS constructed from a cyanostilbene-bridged ditopic UPy donor **M** and ultralow content of acceptor for white-light emission [61], in this work, we further fabricate a sequential two-step energy transfer LHS with tunable emission by using **M**-based SPNPs as a nano-platform. Herein, the SPNPs are formed by

☆ This paper is dedicated to the memory of Prof. Jiang Wei.

* Corresponding authors.
E-mail addresses: xiaotangxin@cczu.edu.cn (T. Xiao), lywang@nju.edu.cn (L. Wang).

https://doi.org/10.1016/j.cclet.2023.108618
1001-8417/

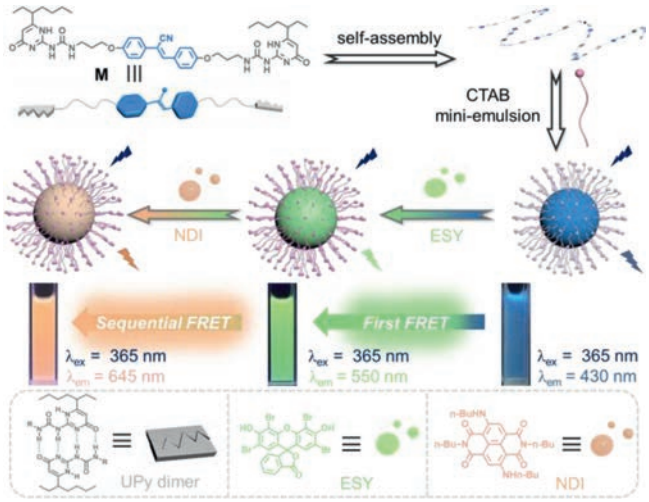

Fig. 1. Cartoon representation of the fabrication of a two-step energy transfer artificial LHS based on supramolecular polymeric nanoparticles.

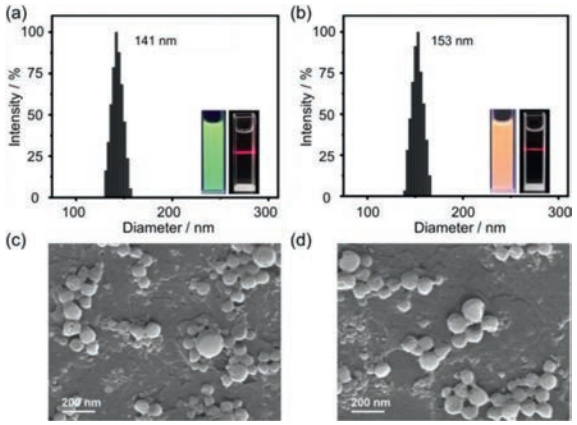

Fig. 2. DLS data of (a) ESY@**M** SPNPs, inset: photographs of ESY@**M** SPNPs under UV irradiation at 365 nm (left) and the Tyndall effect of ESY@**M** SPNPs (right), (b) ESY-NDI@**M** SPNPs, inset: photographs of ESY-NDI@**M** SPNPs under UV irradiation at 365 nm (left) and the Tyndall effect of ESY-NDI@**M** SPNPs (right). SEM images of (c) ESY@**M** SPNPs and (d) ESY-NDI@**M** SPNPs. [**M**] = 5×10^{-5} mol/L, [ESY] = 6.67×10^{-7} mol/L, [NDI] = 4×10^{-7} mol/L, respectively.

quadruple hydrogen bonding and hydrophobic interactions (Fig. 1). The cyanostilbene group endows **M** with AIE property, while the UPy moieties enables itself with quadruple hydrogen bonding ability. Assisted by cetyltrimethyl ammonium bromide (CTAB), SPNPs of **M** can be formed in aqueous media through the mini-emulsion method [62,63]. By incorporating two hydrophobic dyes Eosin Y (ESY) and NDI into the SPNPs as the relay acceptor and the final acceptor, excited energy of **M** (donor) can go through ESY and ultimately achieve to NDI efficiently. Compared with one-step energy transfer systems with linearly tuned emission, the current sequential energy transfer system exhibits a broad range of emission from blue to green to orange upon excitation at a constant wavelength. This light harvesting model may have great potential in understanding the fundamentals of natural photosynthetic system, as well as promoting the development of organic luminescent materials based on hierarchical self-assembly.

The supramolecular polymerization of **M** based on quadruple hydrogen bonds and the AIE property of **M** have been demonstrated previously [61]. SPNPs of **M** in water was fabricated through a supramolecular polymerization followed by mini-emulsion strategy. A solution of **M** (50 μL, 10 mmol/L) in chloroform was dropped into an aqueous solution of CTAB (10 mL, 1.0 mmol/L) followed by ultrasonication for 20 min. The hierarchically self-assembled SPNPs in aqueous media showed a strong blue emission under a UV lamp irradiation due to the AIE effect (Fig. S1 in Supporting information). The absolute fluorescence quantum yield of the SPNPs was determined to be 7.88% (Fig. S2a in Supporting information). These observations indicate that SPNPs of **M** have been successfully prepared with the help of CTAB.

Since **M** shows excellent blue fluorescence as SPNPs dispersed in water, it is reasonable to construct donor-acceptor system by the co-assembly of hydrophobic dyes into the nanosphere of **M**. The hydrophobic dyes ESY and NDI were selected according to their proper photophysical properties (*vide infra*). They could be entrapped inside the SPNPs by mini-emulsifying them with **M** simultaneously. Size of these loaded SPNPs was measured by dynamic light scattering (DLS) and morphology was further characterized by scanning electron microscopy (SEM). DLS of ESY@**M** SPNPs showed a narrow size distribution with an average hydrodynamic diameter of 141 nm (Fig. 2a). SEM image indicated that SPNPs of ESY@**M** exhibit well-defined spherical architecture with diameter of *ca.* 120 nm (Fig. 2c), in a good agreement with DLS measurements. Moreover, the prepared ESY-NDI@**M** SPNPs exhibited a slightly larger particle size of about 153 nm monitored by DLS (Fig. 2b) and also a spherical shape according to SEM (Fig. 2d). Notably, Tyndall effects were obviously observed for both samples, further verifying the formation of abundant nanoaggregates (Fig. 2, insets).

The energy transfer from **M** to ESY (relay acceptor) was investigated due to the considerable overlap between the absorption spectrum of ESY and the emission band of **M** (Fig. 3a). As shown in Fig. 3b, upon the co-assembly of ESY into **M** SPNPs, the fluorescence intensity of **M** at 430 nm decreased remarkably, while the emission of ESY at 550 nm increased significantly ($\lambda_{ex} = 365$ nm). At the same time, the emission color varied from bright blue to yellowish green (Fig. 3c, inset). These observations indicated that energy transfer had taken place from the donor to ESY. Moreover, a considerable decrease of fluorescence lifetime of **M** after co-assembly with ESY further confirms the energy transfer process (Fig. 3c). The lifetime curves showed a double exponential decay for both **M** and ESY@**M** (Table S1 in Supporting information). Fluorescence lifetime of **M** measured at 430 nm shows that $\tau_1 = 0.43$ ns and $\tau_2 = 3.17$ ns. After co-assembled with 2% ESY, fluorescence life-

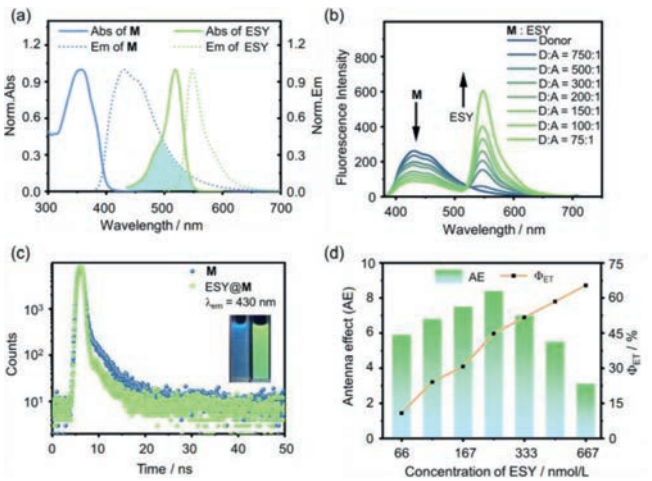

Fig. 3. The first-step energy transfer from **M** to ESY. (a) Normalized fluorescence spectra (dashed curves) of **M** (blue trace) and ESY (green trace), and their corresponding normalized UV–vis spectra (solid curves). (b) Fluorescence spectra of **M** as SPNPs in water with the titration of ESY ([**M**] = 5×10^{-5} mol/L, $\lambda_{ex} = 365$ nm). (c) Fluorescence decay profiles of **M** and ESY@**M**, inset: fluorescence photos of **M** (left) and ESY@**M** (right), [**M**] = 5×10^{-5} mol/L, [ESY] = 6.67×10^{-7} mol/L. (d) Φ_{ET} and AE at different concentrations of ESY.

time of **M** under the same condition decreased to $\tau_1 = 0.24$ ns and $\tau_2 = 2.68$ ns, indicating that the first-step FRET had been certainly realized.

Energy-transfer efficiency (Φ_{ET}) and antenna effect (AE) are usually employed to evaluate the performance of man-made LHS. Φ_{ET} is the quenching rate of the donor after transferring excitation energy to the acceptor, and AE is the amplification of the emission intensity of the acceptor after absorbing excitation energy from the donor. When the molar ratio of **M**/ESY was 75/1, Φ_{ET} was determined to be 65.4% (Fig. S3 and Table S4 in Supporting information). As shown in Fig. 3d, Φ_{ET} increased with the increase of ESY content. In the above case, AE of the system was calculated to be 3.1-fold with an absolute fluorescence quantum yield of 19.05% (Fig. S2b in Supporting information), which is much higher than **M** itself, further indicative of an efficient light harvesting ability of ESY. Notably, the AE value increased remarkably until it reached a maximum of 8.4-fold when **M**/ESY = 200/1 (Fig. 3d and Table S6 in Supporting information). By employing the methoxy–substituted cyanostilbene precursor as a donor and ESY as an acceptor, poor energy-transfer efficiency and antenna effect were observed (Fig. S7 in Supporting information), indicating that the quadruple hydrogen bonded supramolecular polymer is crucial for the construction of the light-harvesting system.

Natural LHS gives us lots of inspirations, for example, it usually consists of multi-type of chromophores and the absorbed energy will go through multiple steps to reach the reaction center. Therefore, we further attempted to construct sequential energy-transfer system based on this SPNP platform. The hydrophobic dye NDI was then chosen as the final acceptor to harvest the excited energy from ESY@**M**, because the normalized UV–vis spectrum of NDI exhibits a considerable overlap with the fluorescence band of ESY (Fig. 4a). When NDI was gradually titrated into the ESY@**M** system, the emission intensity of ESY at 550 nm decreased and the intensity of NDI at 645 nm increased significantly when excited at 365 nm (Fig. 4b). Meanwhile, the emission color was changed from yellowish green to orange red (Fig. 4c, inset). This confirms that ESY could serve as a relay acceptor to obtain excitation energy from **M**, and subsequently transport it to NDI. Notably, NDI might also absorb excitation energy directly from **M** due to a small overlap between **M**'s emission band and NDI's absorption spectrum (Fig. S8a in Supporting information). However, although part of the excitation energy could be absorbed by NDI in the NDI@**M** SPNPs, emission of NDI was hardly observed, indicative of a very poor antenna effect (Fig. S8b in Supporting information). This suggests that ESY, as an energy bridge, is necessary for the two-step sequential energy transfer (Fig. S8c in Supporting information). Fluorescence lifetimes were further measured to confirm the energy transfer process between ESY and NDI. The lifetime curves show a double exponential decay (Fig. 4c). Fluorescence lifetimes of ESY@**M** monitored at 550 nm are determined to be $\tau_1 = 2.52$ ns and $\tau_2 = 9.32$ ns (Table S2 in Supporting information). In contrast, the ESY-NDI@**M** assembly exhibits a dramatic decrease in lifetimes: $\tau_1 = 1.54$ and $\tau_2 = 4.81$ ns, indicating that the two-step sequential energy transfer had indeed taken place.

Φ_{ET} and AE were also calculated to evaluate the second-step light harvesting ability (Fig. 4d). Φ_{ET} was calculated from the emission quenching ratio of ESY at 550 nm. Taking an example with a molar ratio of **M**/ESY/NDI = 750/10/6, Φ_{ET} was calculated to be 88.2% (Fig. S4 and Table S5 in Supporting information). In this case, the absolute fluorescence quantum yield was measured to be 25.3% (Fig. S2c in Supporting information), which is obviously higher than that of ESY@**M**. As shown in Fig. 4d, Φ_{ET} was increased as the NDI content in the system increased. It is noteworthy that the AE value in this case is 26.3 and climbed up to 34.5 with a molar ratio of **M**/ESY/NDI = 750/10/1. Notably, compared with other sequential systems reported recently, the second-step Φ_{ET} and AE in this system are superior (Table S8 in Supporting information). These results further verified that the supramolecular ESY-NDI@**M** SPNPs could serve as an efficient LHS with stepwise energy transfer. Interestingly, these energy-transfer cascade systems show high stability in solution, which can be stored for several weeks without precipitation and photobleaching. This might be attributed to the high fidelity of the multiple hydrogen bonds and the good dispersion ability of the CTAB in water.

The luminescent color variations of the first-step and second-step energy transfer processes could be directly read on the CIE 1931 chromaticity diagram (Fig. 5a). The **M** nanoaggregates located in the blue area. Upon the molar ratio of ESY increased from 750:1 to 75:1, the emission color of the system gradually changed from blue to yellowish green. In the second-step energy transfer, the emission color gradually turned to orange red with the addition of NDI from NDI/ESY/**M** = 1/10/750 to 6/10/750. The triangular emission regions formed by ESY@**M** and ESY-NDI@M

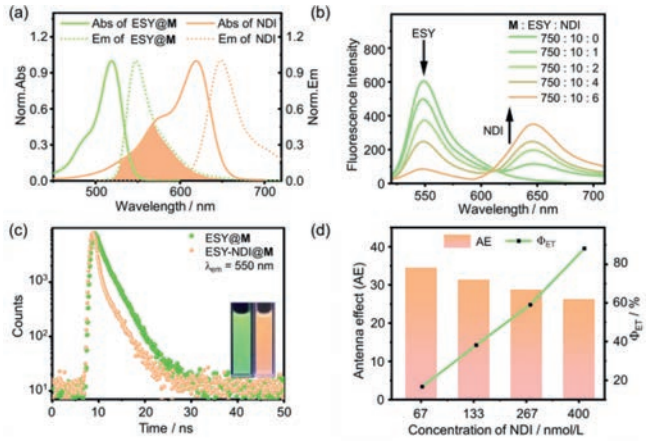

Fig. 4. The second-step energy transfer from ESY to NDI. (a) Normalized fluorescence spectra (dashed curves) of ESY@**M** (green trace) and NDI (red trace), and their normalized UV–vis spectra (solid curves). (b) Fluorescence spectra of ESY@**M** ([**M**] = 5×10^{-5} mol/L, [ESY] = 6.67×10^{-7} mol/L, λ_{ex} = 365 nm) with the titration of NDI. (c) Fluorescence decay profiles of ESY@**M** and ESY-NDI@**M**, inset: fluorescence images of ESY@**M** (left) and ESY-NDI@**M** (right) ([**M**] = 5×10^{-5} mol/L, [ESY] = 6.67×10^{-7} mol/L, [NDI] = 4×10^{-7} mol/L). (d) Φ_{ET} and AE at different concentrations of NDI.

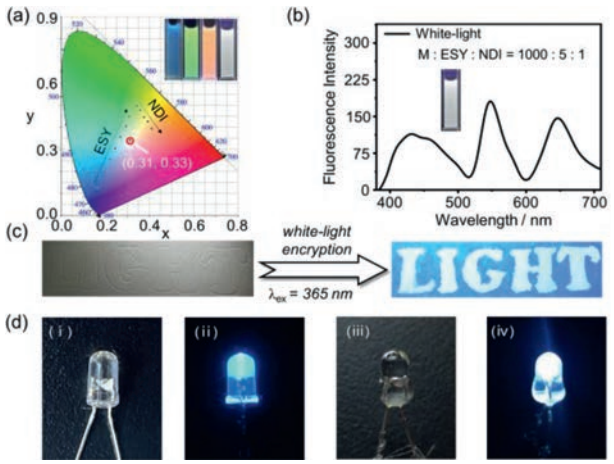

Fig. 5. (a) The CIE chromaticity diagram of emission color variations by adjusting the ratios of the dyes, and the white-light emission coordinate (0.31, 0.33). (b) Fluorescence spectrum of the white-light emission. Inset: white-emission image. (c) Letters painted by a white-light emitting solution, showing the encryption function. (d) Photographs of an uncoated LED bulb and a coated LED bulb before and after illumination.

provides the possibility to create white-light emission materials [64–66]. As expected, a white-light emission was achieved when **M**/ESY/NDI = 1000/5/1 ([**M**] = 5×10^{-5} mol/L) (Fig. 5b). The color coordinate was calculated to be (0.31, 0.33), which is close to the pure white emission (0.33, 0.33). Absolute fluorescence quantum yield of the while-light emission was 19.24% (Fig. S10 in Supporting information). By taking the white-light emission material as ink, no letters could be read out under natural light (Fig. 5c). However, the letters could be clearly readout under UV light, indicating that the system can be utilized as a solid-state encryption material. Moreover, this white-emission material was further used to prepare white LED device (Fig. 5d). A blue LED bulb ($\lambda_{ex} = 365$ nm) was coated with the white-light emission material and then a 3 V bias was applied. As a result, bright white light was generated when turned on the bulb.

In conclusion, a two-step sequential light harvesting system based on supramolecular polymeric nanoparticles was fabricated. Emission of the donor could be greatly enhanced through a hierarchical self-assembly including supramolecular polymerization and mini-emulsion. The prepared nanoparticles are highly emissive and can serve as excellent energy donor, while the hydrophobic dyes ESY and NDI can act as relay and final energy acceptors to harvest excitation energy sequentially. This artificial LHS showed a tunable fluorescence emission including a white-light emission. This study not only provides a general strategy for the construction of stepwise energy-transfer LHSs from supramolecular monomers, but also provides potential applications in aqueous photoluminescent materials.

Declaration of competing interest

The authors declare that they have no known competing financial interests or personal relationships that could have appeared to influence the work reported in this paper.

Acknowledgments

We gratefully thank the financial support from the National Natural Science Foundation of China (No. 21702020). We also acknowledge the analytical testing support from Analysis and Testing Center, NERC Biomass of Changzhou University. L.Z. acknowledges the Postgraduate Research & Practice Innovation Program of Jiangsu Province (No. KYCX22_3012).

Supplementary materials

Supplementary material associated with this article can be found, in the online version, at doi:10.1016/j.cclet.2023.108618.

References

[1] M. Schulze, V. Kunz, P.D. Frischmann, et al., Nat. Chem. 8 (2016) 576–583.
[2] X. Qin, M. Suga, T. Kuang, et al., Science 348 (2015) 989–995.
[3] J. Otsuki, J. Mater. Chem. A 6 (2018) 6710–6753.
[4] S. Guo, Y. Song, Y. He, et al., Angew. Chem. Int. Ed. 57 (2018) 3163–3167.
[5] C. Ma, N. Han, Y. Wang, et al., Chin. Chem. Lett. 34 (2023) 108081.
[6] K. Wang, K. Velmurugan, B. Li, et al., Chem. Commun. 57 (2021) 13641–13654.
[7] Y.X. Hu, W.J. Li, P.P. Jia, et al., Adv. Opt. Mater. 8 (2020) 2000265.
[8] T. Xiao, W. Zhong, L. Zhou, et al., Chin. Chem. Lett. 30 (2019) 31–36.
[9] H.Q. Peng, L.Y. Niu, Y.Z. Chen, et al., Chem. Rev. 115 (2015) 7502–7542.
[10] P.D. Frischmann, K. Mahata, F. Würthner, Chem. Soc. Rev. 42 (2013) 1847–1870.
[11] R. Ziessel, A. Harriman, Chem. Commun. 47 (2011) 611–631.
[12] R. Wang, M. Hao, G. Sun, et al., J. Xihua Univ. Nat. Sci. Ed. 39 (2020) 9–19.
[13] H. Qian, T. Xiao, R.B.P. Elmes, et al., Chin. Chem. Lett. 34 (2023) 108185.
[14] D. Zhang, W. Yu, S. Li, et al., J. Am. Chem. Soc. 143 (2021) 1313–1317.
[15] Y. Li, S.S. Rajasree, G.Y. Lee, et al., J. Am. Chem. Soc. 143 (2021) 2908–2919.
[16] Z. Zhang, Z. Zhao, Y. Hou, et al., Angew. Chem. Int. Ed. 58 (2019) 8862–8866.
[17] T. Xiao, D. Chen, H. Qian, et al., Dyes Pigments 210 (2023) 110958.
[18] T. Xiao, H. Qian, Y. Shen, et al., Mater. Today Chem. 24 (2022) 100833.
[19] G. Sun, L. Cai, H. Cui, et al., Dyes Pigments 201 (2022) 110257.
[20] X.M. Chen, K.W. Cao, H.K. Bisoyi, et al., Small 18 (2022) e2204360.
[21] L. Xu, Z. Wang, R. Wang, et al., Angew. Chem. Int. Ed. 59 (2020) 9908–9913.
[22] X.H. Wang, N. Song, W. Hou, et al., Adv. Mater. 31 (2019) 1903962.
[23] J.J. Li, Y. Chen, J. Yu, et al., Adv. Mater. 29 (2017) 1701905.
[24] P. Ensslen, H.A. Wagenknecht, Acc. Chem. Res. 48 (2015) 2724–2733.
[25] P.K. Dutta, R. Varghese, J. Nangreave, et al., J. Am. Chem. Soc. 133 (2011) 11985–11993.
[26] A. Nandy, S. Mukherjee, J. Phys. Chem. Lett. 13 (2022) 6701–6710.
[27] Q. Song, S. Goia, J. Yang, et al., J. Am. Chem. Soc. 143 (2021) 382–389.
[28] S. Hirayama, K. Oohora, T. Uchihashi, et al., J. Am. Chem. Soc. 142 (2020) 1822–1831.
[29] F. Würthner, Angew. Chem. Int. Ed. 59 (2020) 14192–14196.
[30] Y. Hong, J.W.Y. Lam, B.Z. Tang, Chem. Soc. Rev. 40 (2011) 5361–5388.
[31] Y.X. Yuan, J.H. Jia, Y.P. Song, et al., J. Am. Chem. Soc. 144 (2022) 5389–5399.
[32] T. Xiao, C. Bao, L. Zhang, et al., J. Mater. Chem. A 10 (2022) 8528–8534.
[33] C.Q. Ma, X.L. Li, N. Han, et al., J. Mater. Chem. A 10 (2022) 16390–16395.
[34] X. Zhu, J.X. Wang, L.Y. Niu, et al., Chem. Mater. 31 (2019) 3573–3581.
[35] Y. Li, Y. Dong, L. Cheng, et al., J. Am. Chem. Soc. 141 (2019) 8412–8415.
[36] W. Zhang, Y. Luo, X.L. Ni, et al., Chem. Eng. J. 446 (2022) 136954.
[37] Y. Li, C. Xia, R. Tian, et al., ACS Nano 16 (2022) 8012–8021.
[38] T. Xiao, L. Zhang, H. Wu, et al., Chem. Commun. 57 (2021) 5782–5785.
[39] P.P. Jia, L. Xu, Y.X. Hu, et al., J. Am. Chem. Soc. 143 (2021) 399–408.
[40] G. Sun, W. Qian, J. Jiao, et al., J. Mater. Chem. A 8 (2020) 9590–9596.
[41] J.J. Li, H.Y. Zhang, X.Y. Dai, et al., Chem. Commun. 56 (2020) 5949–5952.
[42] M. Hao, G. Sun, M. Zuo, et al., Angew. Chem. Int. Ed. 59 (2020) 10095–10100.
[43] L. Ji, Y. Sang, G. Ouyang, et al., Angew. Chem. Int. Ed. 58 (2019) 844–848.
[44] T. Xiao, J. Wang, Y. Shen, et al., Chin. Chem. Lett. 32 (2021) 1377–1380.
[45] T. Xiao, L. Zhou, X.Q. Sun, et al., Chin. Chem. Lett. 31 (2020) 1–9.
[46] M. Wehner, F. Würthner, Nat. Rev. Chem. 4 (2020) 38–53.
[47] E. Krieg, M.M.C. Bastings, P. Besenius, et al., Chem. Rev. 116 (2016) 2414–2477.
[48] L. Yang, X. Tan, Z. Wang, et al., Chem. Rev. 115 (2015) 7196–7239.
[49] X. Yan, F. Wang, B. Zheng, et al., Chem. Soc. Rev. 41 (2012) 6042–6065.
[50] T. Aida, E.W. Meijer, S.I. Stupp, Science 335 (2012) 813–817.
[51] X.H. Wang, X.Y. Lou, T. Lu, et al., ACS Appl. Mater. Interfaces 13 (2021) 4593–4604.
[52] Y. Han, X. Zhang, Z. Ge, et al., Nat. Commun. 13 (2022) 3546.
[53] T. Aida, Adv. Mater. 32 (2020) e1905445.
[54] R.P. Sijbesma, F.H. Beijer, L. Brunsveld, et al., Science 278 (1997) 1601–1604.
[55] T. Xiao, W. Zhong, W. Yang, et al., Chem. Commun. 56 (2020) 14385–14388.
[56] K.X. Teng, L.Y. Niu, N. Xie, et al., Nat. Commun. 13 (2022) 6179.
[57] T. Xiao, L. Zhou, L. Xu, et al., Chin. Chem. Lett. 30 (2019) 271–276.
[58] T. Xiao, L. Xu, L. Zhou, et al., J. Mater. Chem. B 7 (2019) 1526–1540.
[59] M. Cheng, D. Chen, L. Zhang, et al., Org. Chem. Front. 10 (2023) 1380–1385.
[60] T. Xiao, L. Tang, D. Ren, et al., Chem. Eur. J. 29 (2023) e202203463.
[61] K. Diao, D.J. Whitaker, Z. Huang, et al., Chem. Commun. 58 (2022) 2343–2346.
[62] C.L. Sun, H.Q. Peng, L.Y. Niu, et al., Chem. Commun. 54 (2018) 1117–1120.
[63] H.Q. Peng, J.F. Xu, Y.Z. Chen, et al., Chem. Commun. 50 (2014) 1334–1337.
[64] D. Li, J. Wang, X. Ma, Adv. Opt. Mater. 6 (2018) 1800273.
[65] X. Zhang, D. Görl, F. Würthner, Chem. Commun. 49 (2013) 8178–8180.
[66] H.T. Feng, X. Zheng, X. Gu, et al., Chem. Mater. 30 (2018) 1285–1290.